

Geochemistry of the Kuiseb metasediments around Windhoek, Namibia

G.N. Phillips¹, D.I. Groves² and K. Reed

Department of Geology, University of the Witwatersrand, WITS 2050, South Africa

The metasediments of the Kuiseb Formation around Windhoek are a highly deformed and metamorphosed sequence of interlayered psammitic and pelitic gneisses and schists. A well-developed tectonic fabric is parallel to lithological layering and is itself deformed in local shear zones and by a locally developed crenulation cleavage. The gneisses and schists are interlayered on all scales from a few centimetres to tens of metres. The schists are associated with veining and retrogression of the peak metamorphic assemblage of biotite - muscovite - plagioclase - chlorite - garnet - quartz. East of Windhoek, the gneisses and schists of the Kleine Kuppe Formation (underlying the Kuiseb Formation) are distinguished from the latter by their higher Nb and La contents, lower Y, Zn and V, and the presence of kyanite and staurolite: otherwise the geochemistry and mineralogy of the two formations is rather similar. Within the Kuiseb Formation, the gneisses are lower in all elements except Si, Ca, Na, Sr and Zr, compared to the schists. Ratios of Nb, P, La, Ce, Y and Fe, with Ti are virtually constant through the dataset, not being significantly different between the gneisses and schists. However, Al/Ti and Ti/Zr are higher in the schists. These data are compatible with a single dominant clay phase at deposition, along with variable quartz and possible minor detrital zircon. The data also suggest negligible mobility of Ti, Nb, P, La, Ce, Y and Fe after burial, and further imply that original sandy and shaley units cannot be distinguished on the basis of these immobile elements. Mobility of Si, Mn, Mg, K, Rb, Ba, Cu, Ni, Zn, Co, V and Cr is implied: Ca, Na and Sr may reflect a feldspar detrital component and/or mobility of these elements after burial. The layering defined by gneisses and schists appears to have resulted from lithological differences (possibly slight) that have been accentuated by later deformation and fluid infiltration.

Introduction

The Kuiseb Formation comprises pelitic, semi-pelitic and psammitic gneisses and schists at the top of the Swakop Group which crop out over a large area of central Namibia (Fig. 1). The monotonous nature of the sequence and its vast extent have presented difficulties in subdivision of the succession, in determination of the detailed depositional environment, and in determining the nature of precursors. Geochemical studies are used here to supplement stratigraphic and petrological attempts to answer the above questions.

Deformation and metamorphism have affected the whole sequence, overprinting sedimentary textures and leading to significant veining, cleavage formation and metamorphic layering. These features indicate that isochemical metamorphism cannot be assumed and, instead, the mobility of some elements (e.g. Si, alkalis) appears likely.

The aim of this study is to characterize the Kuiseb metasediments in a small area around Windhoek, and to evaluate the application of geochemistry in their subdivision and the determination of their depositional and post-depositional history. The area around Windhoek was specifically chosen since sections of continuous exposure are available and several road cuttings enable the effects of weathering to be minimized. The study is designed to complement other projects within the Kuiseb Formation that are of a more regional nature.

The use of carefully field-controlled samples has allowed the testing of simple sedimentary models against

existing whole-rock geochemical compositions.

Regional setting

The Kuiseb Formation in the Windhoek area is situated in the north-east trending Khomas Trough (80 x 400 km) which occurs within the late Proterozoic Damara Orogen of central Namibia near its southern edge (Fig. 1). The southeastern boundary of the Khomas Trough is marked by the Southern Margin Zone (Hoffmann, 1983) of older metasediments and meta-igneous rock types. Immediately underlying the Kuiseb Formation is the Kleine Kuppe Formation, and schists in these two groups are difficult to distinguish in hand specimens. The Kuiseb schists north of Windhoek have been sampled in the past from variably weathered trenches, and composites have been analysed for major elements (Miller *et al.*, 1983). From plots involving K₂O, SiO₂, Na₂O, MgO and Al₂O₃, an acid igneous source area was inferred on the basis of the high K₂O, and these data were used to suggest zones of differing "maturity".

Metamorphism of the Kuiseb metasediments has produced chlorite, garnet and biotite over wide areas, and is inferred to increase from upper greenschist to lower amphibolite facies northwards. Assemblages that tightly constrain pressure or temperature are scarce in most parts of the Khomas Trough.

Description of the Kuiseb and Kleine Kuppe Formations

Samples of Kuiseb metasediments were collected from six road localities up to 20 km west of Windhoek (Table 1 Appendix; Figs 1 and 2). For the purpose of the study, the more psammitic types are referred to as "gneisses" (although not all were strictly gneissic), and

Present addresses:

¹Key Centre in Economic Geology, Geology Department, James Cook University, Townsville, 4811, Qld, Australia

²Key Centre for Strategic Mineral Deposits, Department of Geology, University of Western Australia, Nedlands 6009, WA, Australia

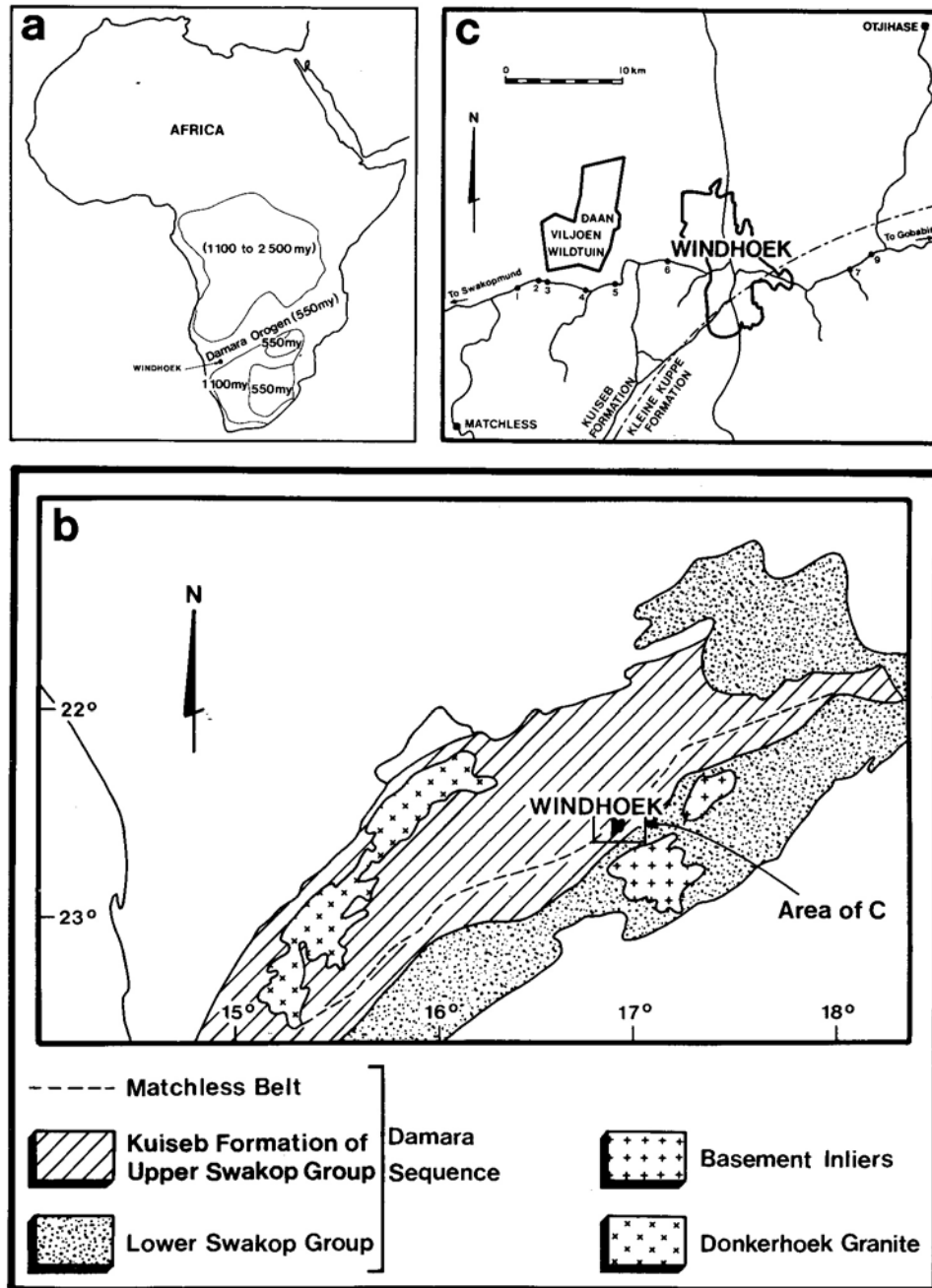


Fig. 1: Composite locality map showing (a) Damara Orogen and Windhoek, (b) the Khomas Trough, Kuseib Formation and Matchless Belt, and (c) roads around Windhoek with the study localities.

the more pelitic types referred to as “schists”. Sketches and photographs of each locality were used to supplement sampling and structural readings (Figs 2 and 3). Further localities east of Windhoek were used to sample gneiss and schist of the underlying Kleine Kuppe Formation (Hoffmann, 1983), and to use these for comparison with the Kuseib Formation. Sampling was designed to obtain the freshest samples from each locality, and to deliberately avoid quartz veining (although its presence was carefully noted). Much of this quartz veining was inferred to have come from local remobilization of silica during metamorphism.

Considerable emphasis was placed on the distribution of gneissic and schistose lithologies. Variations between psammitic gneiss and pelitic schist were mapped out in each locality, and packages of predominantly one type or the other were recognized on three different scales, i.e. several metres (Fig. 3a), several decimetres (Fig. 3b-c), and several centimetres (Fig. 3d-f). In all localities, both gneisses and schists were present. Sampling of the coarser units (metre-scale layering) was by lines of chip samples across compositional layering.

A strong east-west foliation (s_0/s_1) is defined by alternating pelitic and psammitic lenses and by a preferred

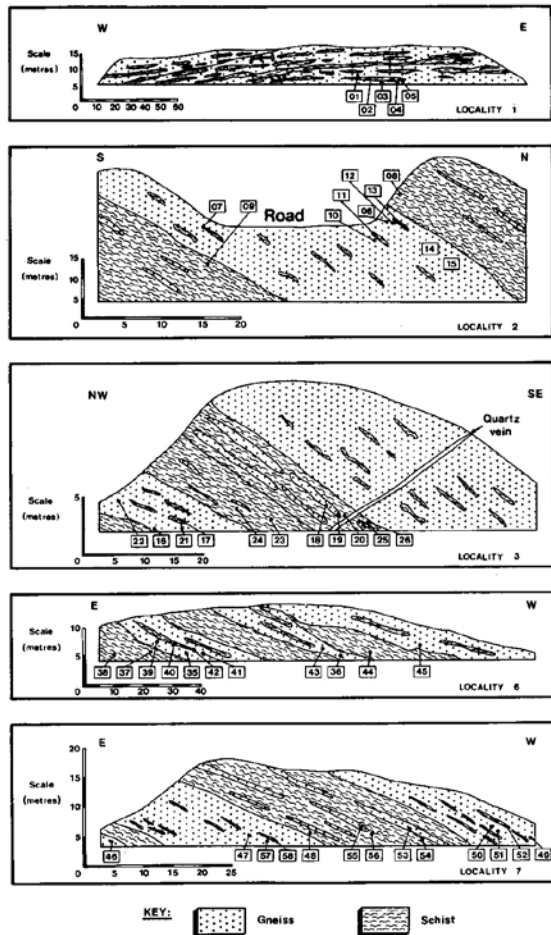


Fig. 2: Sketch maps of five localities to show the different scales of layering between gneisses and schists. The numbers shown on the sketches indicate sampling sites and correspond to the last two digits of analysis numbers listed in Tables 2-6.

orientation of micas. This foliation trends near-parallel to the length of the Khomas Trough, and the dip of the foliation is usually from 20 to 40 degrees to the north (e.g. strike 075/ dip 40 N at locality 1, 070/30 N to 090/45 N at locality 5, 100/50 N to 125/25 N at locality 6, 070/30 N at locality 7). The s_0/s_1 foliation is commonly preserved in gneissic layers, but overprinted by a strong shear foliation (s_2) associated with quartz veining in the more schistose layers (Fig. 3g).

Near-isoclinal folds defined by the dominant s_0/s_1 layering are locally preserved in the more gneissic layers. A weakly developed crenulation cleavage overprints the main east-west cleavage in the more schistose layers, and strikes approximately north-south and dips 20-40 degrees to the west. A lineation associated with the crenulation plunges 30 degrees to the north-west.

The gneisses form 20-30% of exposed rock types and make up the more resistant east-west trending ridges. The dominant minerals are quartz, plagioclase and biotite (15%) with minor to negligible white mica, garnet, chlorite, apatite, zircon, epidote and tourmaline. Alternating micaceous and quartzose layers define the gneissosity. Retrogression mainly involves pseudomorphism

of biotite by chlorite and white mica, with some late carbonates.

The minerals in the schists are the same as those in the gneisses, but the proportions are quite different and more variable. Biotite, muscovite, chlorite and quartz occur in approximately similar abundances, tourmaline is widespread, and garnet relatively common (Fig. 4). In this study, kyanite and staurolite were only recorded in the Kleine Kuppe Formation east of Windhoek (cf. Kasch, 1983). Retrogression to chlorite-rich schist is common.

Conditions of at least upper greenschist facies are indicated on the basis of the stable phases west of Windhoek, with temperatures above 400°C being inferred. Interpolation of the more extensive synthesis of Kasch (1983), covering all of the Khomas Trough, would suggest amphibolite facies conditions were reached around Windhoek.

Some quartzo-feldspathic lenses occur fit the western end of locality 1 in high-strain schistose zones, and/or adjacent to quartz veins and biotite-rich schists. These have approximately equal proportions of quartz and feldspar and subordinate white mica. These lenses have a composition that appears appropriate for partial melt segregations (probably externally derived), but they have not been studied in detail.

Geochemistry

Samples from six road cuttings were collected for whole-rock analysis, reduced in a jaw crusher and tungsten carbide mill, and prepared as pressed pellets and fused disks for XRF analysis of major and minor elements in the Department of Geology, University of the Witwatersrand. Each sample was prepared and analysed in duplicate, and all samples were analysed in one analytical run to ensure high precision of data and valid comparison between samples. The method of preparation may have introduced contamination by W and Co, warranting certain cautions with the Ni and Co concentrations. Results for all analysed samples are presented (Table 2 - Appendix) with the locality, rock type (whether psammitic gneiss or pelitic schist), the identification number of the set of closely spaced samples, and the scale of layering represented by each sample.

Kuiseb metasediments

The Kuiseb metasediments are dominated by SiO_2 , Al_2O_3 , FeO and MgO with significant TiO_2 , CaO, Na_2O and especially K_2O (Table 2). Although variations in most major elements are relatively small, K_2O and minor elements vary by a factor of two to three within the dataset. One concern of this study was to determine the origin of this geochemical variation and relate it, if possible, to the different scales of lithological layering.

Thirty-three analyses of gneisses and schists (Table 3 - Appendix, average analyses A and B) demonstrate

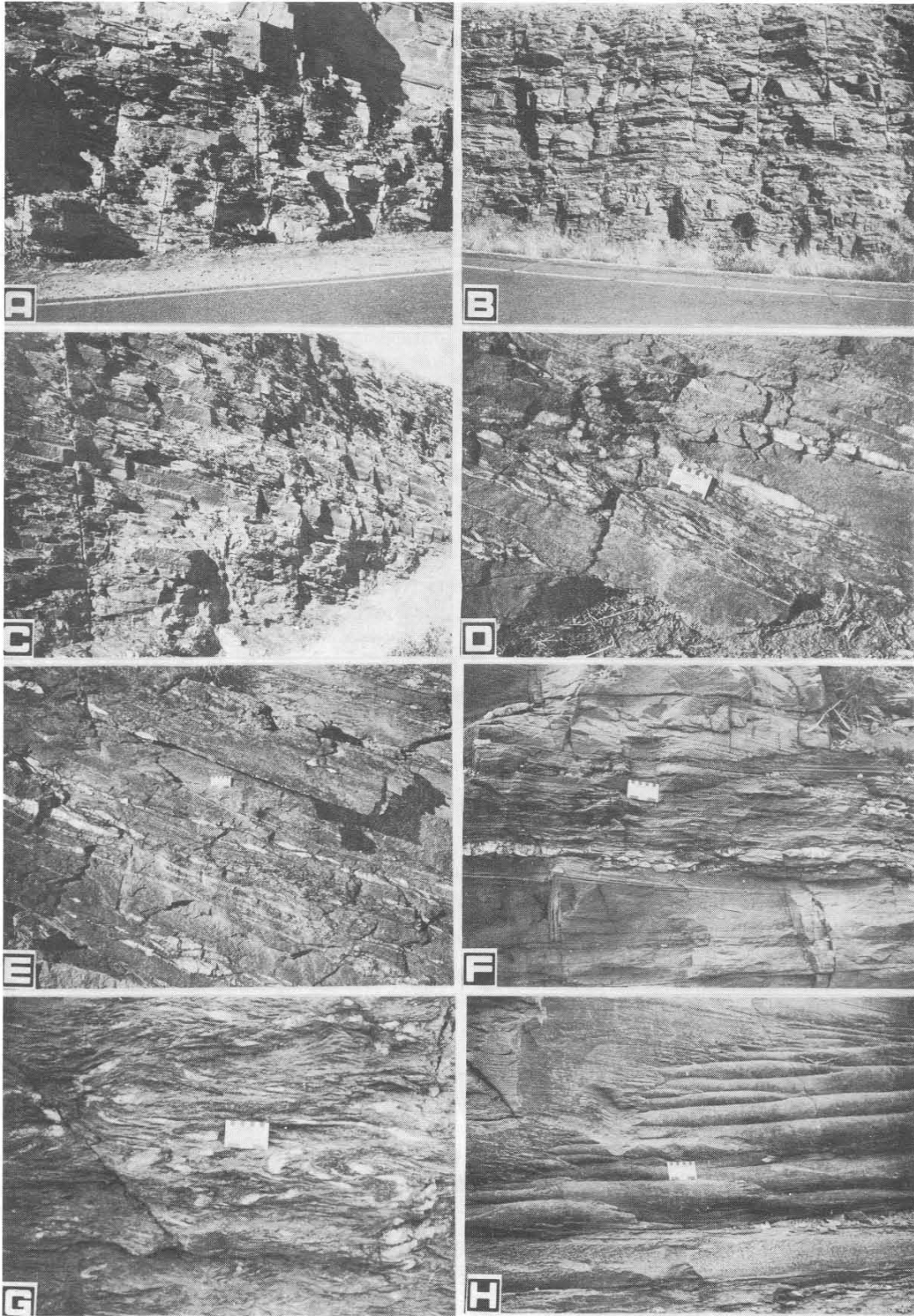


Fig. 3: Composite of field photographs showing (a) metre-scale layering of pelitic schists along road edge, and psammitic gneiss in the upper right corner: locality 7; (b) exposure of thick gneissic units and better-layered schistose units with quartz veining, locality 7.2 km west of bypass, west of Windhoek; (c) decimetre-scale interlayering of gneisses and schists at locality 6; (d) high-strain schist zone with well-developed quartz veining, contrasting with the lack of quartz veining in adjacent gneissic layers, locality 7; (e) high-strain schist zone with quartz veins, all within less-strained gneiss in locality 7; (f) quartz veins in foliated biotite schist, locality 1; (g) crenulation (kink) folds defined by quartz veins in schist, locality 9; (h) mullion development on joint surface, locality 1. The heights of the cuttings shown in a-c are approximately 3-4 metres.

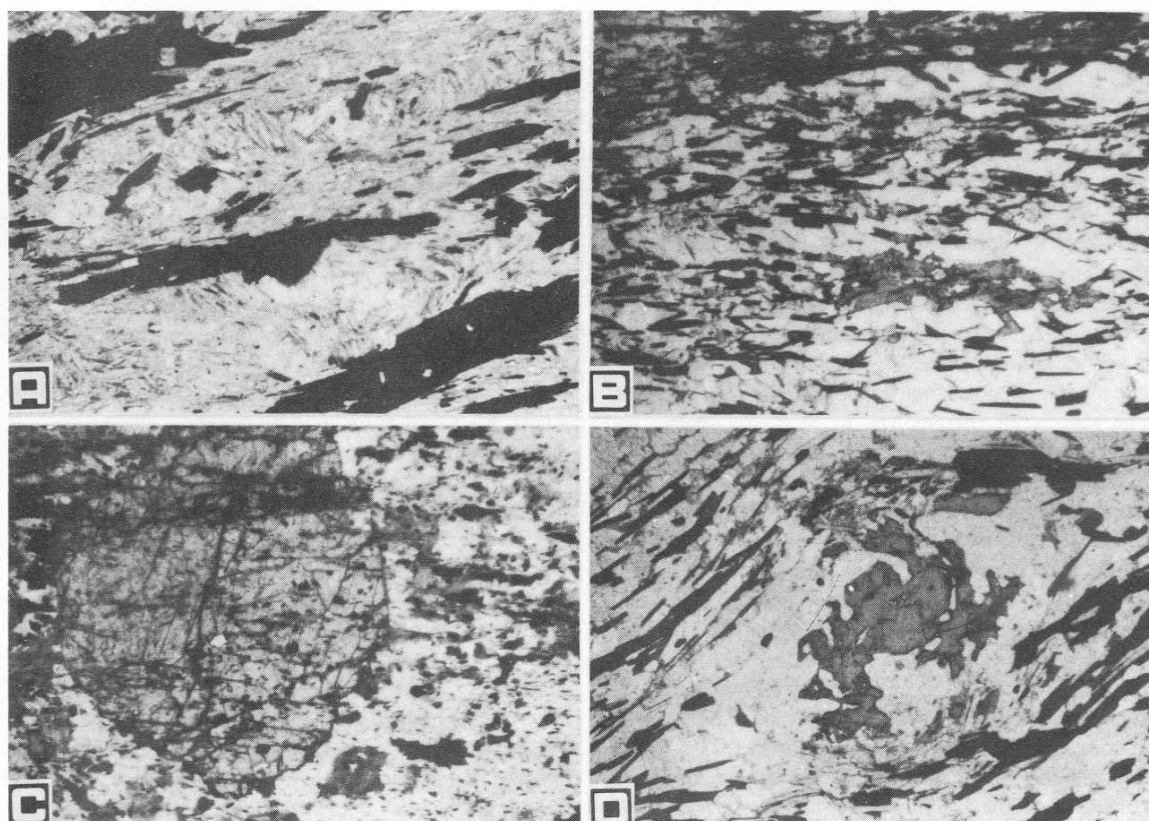


Fig. 4: Composite of photomicrographs showing (a) crumpled biotite - muscovite schist with minor chlorite; (b) biotite schist with muscovite, chlorite, quartz and minor feldspar; (c) late garnet overgrowing mica fabric in schist; (d) relic garnet wrapped around by mica fabric of schist.

higher SiO_2 in the gneisses, and higher concentrations of most other elements in the schists. CaO, Na_2O , Sr and Zr are exceptions as they are higher in the gneisses. There are relatively minor differences within the Kuiseb Formation suite, once allowance is made for the differences between gneisses and schists. Comparison of gneisses and schists from the different scales of layering suggests that the same qualitative differences exist between the two rock types, regardless of whether they are layered on the scale of centimetres, decimetres or several metres (Table 3, compare E and F, G and H, I and J). The differences between gneisses and schists are more accentuated where the layering is on a finer scale, but this may be influenced by the sampling procedure and averaging effect of rows of chip samples in thick units.

Kleine Kuppe metasediments

Samples from the Kleine Kuppe Formation (location 7) are noticeably different from the Kuiseb metasediments west of Windhoek (Table 3, compare A and C, B and D).

The gneisses from the Kleine Kuppe Formation have higher SiO_2 (mean 77%, cf. 72% in the Kuiseb gneisses) and, as a result, other major elements such as Al, Ti, Fe, Mg and P are slightly lower. Higher La and Nb,

with lower Y, Cu, Zn, V and Cr also characterize the Kleine Kuppe gneisses. These differences cannot be adequately explained by silica dilution alone.

The schists from the Kleine Kuppe have higher Ti, Rb, Zr, Ce, La and Nb, with lower Y, Zn and V than the Kuiseb schists. Hence, both gneisses and schists from the Kleine Kuppe Formation have higher Nb and La with lower Y, Zn and V than corresponding rocks from the Kuiseb Formation.

Geochemical interpretation

The systematic differences between gneisses and schists are broadly those that would be expected from an interbedded succession of psammitic and pelitic rocks. Clay-rich, fine-grained sediments (now schists) have an abundance of most major and minor elements associated with the clay minerals, and all these elements decrease (as does Al) with the addition of a silt to sand component (presumably in the form of detrital quartz). The elements enriched along with silica in the gneisses are most reasonably accounted for by some detrital and/or diagenetic feldspar (Na, Ca, Sr) and zircon (Zr).

A similar pattern involving an antithetic relationship of most elements with silica could be generated by heterogeneous extraction of silica from a uniform sequence to form quartz veins and residual schistose

rocks enriched in all immobile elements.

The geochemical data are now explored to ascertain their value in constraining the precursors to the sequence, and the nature of any post-depositional changes.

Principles of geochemical data analysis

In a system with a constant starting composition (i.e. uniform lithology), the ratios of completely immobile elements will remain the same during alteration, weathering or quartz vein formation. Rare-earth elements are commonly used to constrain mobility, but other readily analysed elements are equally suitable. A similar situation of constant ratios may still exist in a two-component system (e.g. silt and clay) if the immobile elements are totally associated with one of the components only (e.g. clay fraction). However, if the immobile elements occur in more than one starting component, a mixing trend involving their ratios will be established prior to burial; interpretation of the geochemical history will be substantially more difficult in such a situation.

The high field-strength elements (small size, high charge) including Ti, Al, Y and Nb, were selected as being most likely to represent the clay fraction of the Kuiseb metasediments prior to burial, and to have remained immobile during metamorphism. Zn has been included as a representative transition metal element that would tend to concentrate strongly in the clay fraction of sediments.

It should be noted that large-ion lithophile elements (large size, small charge) tend to be highly mobile and display similar behaviour within their group: as a result, they may be strongly correlated also, and display constant interelement ratios (K, Rb, Ba) that result from their introduction after burial (not their immobility).

Tabulation of selected element ratios with Ti (Table 4 - Appendix) demonstrate a substantial variation of the ratio within the sample set for V/Ti, small variations for Zr/Ti, Zn/Ti and Al/Ti, and essentially constant ratios for Nb/Ti and Y/Ti. The results also indicate higher Zr/Ti and Nb/Ti, and lower Zn/Ti and V/Ti within the Kleine Kuppe Formation compared to the Kuiseb metasediments. These data imply mobility of at least some of the elements being considered in Table 4, and/or a very complex original sediment.

Test of binary quartz - clay mixing

The most straightforward premise, is that the gneisses and schists represent a continuum from metamorphosed sands through silts to shales, with variable proportions of quartz and a uniform clay mineral. Such a premise implies near-constant ratios between all the elements in the clay mineral at the time of burial, and therefore constant ratios between immobile elements in the current sample set. The Kleine Kuppe metasediments are disregarded from the following discussion because they

have demonstrably different inter-element ratios, almost certainly as a function of deposition and source processes.

For ease of manipulation and illustration, Nb, P, La, Ce, Y, Fe, Al and Zr are expressed relative to constant Ti (Table 5 - Appendix): this does not assume Ti was constant, instead it allows testing of whether part of this group including Ti could have been immobile.

Although this group includes nine major and minor elements there is remarkably little variation in the inter-element ratios (Table 5). For gneisses and schists combined, standard deviations are less than 20% of the means for all ratios. More importantly, gneisses and schists are virtually indistinguishable on the basis of Nb/Ti, P/Ti, La/Ti, Ce/Ti, Y/Ti or Fe/Ti. Al/Ti is higher in schists, and Zr/Ti somewhat lower.

To sustain a model of simple "quartz-one clay" mixing from the present data requires minor mobility of Al, and variability in Zr at the sedimentary stage (due perhaps to minor detrital zircon). Otherwise the constant ratios involving Ti, Nb, P, La, Ce, Y and Fe are compatible with immobility of these elements and one clay phase.

A "quartz-one clay" model also requires mobility of several elements including Mn, Mg, Rb, Ba, Cu, Ni, Zn, Co, V and Cr. In this scenario, all these elements except Mn and Cu would have been added to the schists during alteration. Ca, Na and Sr patterns can be explained by detrital feldspar and/or their mobility during alteration.

With regard to being modelled by one dominant clay, the Kuiseb metasediments are somewhat similar to, say, the metapelites ("shales") of the Witwatersrand Supergroup of South Africa which can be modelled successfully by quartz and a single clay (Phillips, 1988): interestingly, the Witwatersrand shales which show strong coherence between Al, Ti, Nb, Cr, V, P, La and Ce, also show slight scatter of Al/Ti at high Al, with particularly tight Nb/Ti ratios.

Test of complex mixing of two clays and quartz

Realistic sedimentological models could postulate a mixture of quartz and clay from one source and a different clay from another source to explain the variation in the Kuiseb metasediments. Such a sequence would show systematically varying ratios between immobile elements that were sited in both clay phases.

There is little evidence within the elements considered in Table 5 for the presence of a second clay phase, excepting the variable Al/Ti. If this is not due to Al mobility (see above), it is most easily explained by a second clay phase containing Al but not Nb, P, La, Ce, Y or Fe. Minor kaolinite in the finer grained sediments along with a more abundant clay phase throughout, may explain the ratios in Table 5; but it would still be necessary to infer mobility of various elements including Mn, Mg, Rb, Ba, Cu, Ni, Zn, Co, V and Cr.

Behaviour of some major elements

Among the major elements, a negative correlation between Si and Al, and between Si and K, relates to variable proportions of micas in the gneisses and schists. Although a cut-off at 66% SiO₂ will separate these two groups, variations in Si, Al and K within each group suggest a continuum.

A positive correlation exists between K and both Rb and Ba, presumably as a result of their mutual involvement in alteration processes after burial (Table 6 - Appendix). Given the antithetic relationship between Al and Si, and between K and Si, the K-Rb-Ba association suggests that the amount of introduced K (and Rb and Ba) is controlled by the original Al content of the host. In turn, this is inversely related to the proportion of silica.

The K/Rb ratios in gneiss and schist differ significantly (Table 6) suggesting more than one source, or period of introduction, of alkalis: it is believed that this difference relates to original K-Rb-Ba contributions from detrital feldspar combined with alkalis introduced later during alteration.

Given the mobility of Ca, Na and K it is not possible to demonstrate that there was detrital feldspar on the basis of geochemistry.

Relationship of the Kleine Kuppe metasediments to the Kuiseb Formation

The significant difference in geochemistry between rocks from locality 7 and those to the west of Windhoek is support for their separation into different stratigraphic sequences (Hoffmann, 1983). The higher Nb and La, in particular, probably reflects a significant difference in the amount, and hence the source, of minor mineral phases. Interestingly, the behaviour of most elements with respect to the different scales of layering is not significantly different in the Kuiseb and the Kleine Kuppe Formations.

Origin of the layering

The structural, textural and geochemical data suggest that there is little difference (except for scale) between the gneiss - schist layering on the scale of centimetres, decimetres and metres: it also appears that the layering in the Kleine Kuppe Formation is very similar to that in the Kuiseb Formation.

The strong development of the shear fabric in the schists and not the gneisses suggests that either:

(i) an originally homogeneous sequence developed zones of high strain that became loci of fluid flow and alteration which in turn generated the schists from similar precursors to the gneisses, or

(ii) the schists were original heterogeneities in the sequence that accommodated later strain, as well as being fluid channel ways and zones of alteration.

Interestingly, the inferred immobile elements (Ti, Nb, P, La, Ce, Y and Fe) provide no evidence to separate these two possibilities. The constant ratios involving these elements are compatible with either (i) or (ii) above.

Furthermore, based on their chemical properties, other major elements (Si, Mn, Mg, Ca, Na and K) are likely to have been mobile after burial, and this is supported by the data. A similar situation holds for a number of minor elements (Rb, Sr, Ba, Cu, Ni, Zn, Co, V and Cr).

The only geochemical evidence actively favouring the schistose units being originally more shaley, i.e. option (ii), is higher Zr in the gneisses which appears more likely to be original rather than a result of any Zr mobility. If Al was immobile (something not possible to demonstrate from the present dataset), it too would support the schists being originally more shaley units.

Given that the schists are now tectonized and do not preserve sedimentary features, it is not valid to infer from field and mineralogical criteria alone that they are a different starting lithology to the gneisses. Much of the layering between gneisses and schists can be attributed to higher strain, greater fluid access, greater introduction of Mg, K, Rb, Ba, Ni, Zn, Co, V and Cr, and loss of silica to quartz veins, in the layers that are now schists. Based on the Zr and Al data, this greater strain and fluid flux probably concentrated along original heterogeneities. The age of the alteration is likely to be metamorphic (peak or retrograde) and synchronous with deformation, although some element mobility during diagenesis (e.g. alkalis) cannot be ruled out.

Conclusions

The geochemical data are compatible with widespread element mobility after burial, that has involved Mg, Mn, K, Rb, Ba, Cu, Ni, Zn, Co, V, Cr, and probably Ca, Na and Sr. The geochemistry of the sample set approximates simple sedimentary mixing of quartz and one clay component, allowing for minor detrital zircon.

The layering of gneisses and schists appears to be morphologically similar in petrographic and geochemical terms regardless of whether it is on centimetre, decimetre or metre scale. The schists probably represent originally more pelitic layers that have been preferred loci for later strain, fluid flow and alteration, but much of their present contrast with the gneisses is due to alteration processes after burial.

Acknowledgements

Financial support from the Geological Survey of Namibia is gratefully acknowledged, as is the cooperation and support of its Director, Dr R. McG. Miller and his staff. Prof S.E. Maske, Prof T.S. McCarthy, Dr K. Maiden and Mrs S. Hall of the University of the Witwatersrand are thanked for their contributions. G. Balkwill,

G. Borg, J. Breitkopf, G. Henry and K.H. Hoffmann contributed to our understanding of the geology of the Kuiseb schists and surrounding parts of Namibia.

F. Hock is thanked for compilation of the plates, and Drs R. McG. Miller and R. Jacob for their thorough and constructive comments on the manuscript particularly regarding the stratigraphic aspects.

References

- Hoffmann, K.H. 1983. Lithostratigraphy and facies of the S wakop Group of the Southern Damara Belt, SWA/Namibia. *Spec. Publ. geol. Soc. S. Afr.*, **11**, 43-63.
- Kasch, K.W. 1983. Regional P-T variations in the Damara Orogen with particular reference to early high-pressure metamorphism along the Southern Margin Zone. *Spec. Publ. geol. Soc. S. Afr.*, **11**, 243-253.
- Miller, R. McG., Barnes, S-J. and Balkwill, G. 1983. Possible active margin deposits within the Southern Damara Orogen: The Kuiseb Formation between Okahandja and Windhoek. *Spec. Publ. geol. Soc. S. Afr.*, **11**, 73-88.
- Phillips, G.N. 1988. Widespread fluid infiltration during metamorphism of the Witwatersrand goldfields: generation of chloritoid and pyrophyllite. *J. metamorphic Geology*, **6**, 311-332.

Appendix

TABLE 1: Sampling locations.

Cuttings along the road from Windhoek west towards the Matchless mine turnoff. Distances measured from the bypass, west of Windhoek.
 Locality 1: 18.7 km
 Locality 2: 16.5 km
 Locality 3: 16 km
 Locality 4: 11.8 km
 Locality 5: 8.8 km
 Locality 6: 2.1 km
 Cuttings along the road east from Windhoek towards the airport. Distances measured east from Gobabis Rd turnoff in Windhoek.
 Locality 7: 4.1 km
 Locality 9: 6.5 km

Key to tabulated data:
 L: refers to the location of the cutting - numbered from west to east (see Table 1).
 R: refers to rock type - gneiss or schist
 P: refers to the pairing of closely-spaced samples. See also the sketches of each cutting (Fig. 2).
 S: refers to the scale of layering, metres, decimetres or centimetres

TABLE 2: Whole-rock analyses of gneisses and schists from around Windhoek. Total Fe as FeO.

No.	3601	3602	3603	3604	3605	3606	3607	3608	3609	3610	3611	3612	3613	3619
L	i	l	l	l	l	2	2	2	2	2	2	2	2	3
R	g	s	g	g	s	g	g	s	s	g	s	g	s	g
P	1	1	1	2	2	3	3	3	3	4	4	5	5	6
S	C	C	C	C	C	M	M	M	M	C	C	C	C	D
SiO ₂	67.05	52.23	66.24	70.66	54.02	71.06	75.31	61.98	64.27	75.12	57.07	76.10	54.19	69.64
TiO ₂	.99	1.34	.98	.89	1.15	.81	.90	1.08	.90	.74	1.15	.69	1.14	.89
Al ₂ O ₃	13.97	21.15	14.64	12.72	21.50	12.26	10.49	16.25	15.10	10.43	19.52	10.26	20.74	12.59
FeO	5.50	7.86	5.81	5.01	6.99	5.12	4.55	6.76	6.46	4.49	7.13	4.18	7.70	5.52
MnO	.07	.08	.06	.06	.07	.08	.09	.10	.14	.08	.11	.08	.10	.10
MgO	2.58	3.83	2.58	2.40	3.20	2.72	1.65	3.39	3.37	1.98	3.60	1.84	4.15	2.61
CaO	1.42	.98	1.24	.88	.53	1.13	1.25	1.31	1.14	1.16	1.20	1.20	.78	1.65
Na ₂ O	2.13	1.00	1.98	1.35	.64	2.22	2.50	1.70	1.47	2.49	1.52	2.38	.85	2.34
K ₂ O	2.76	6.15	3.35	3.04	6.46	2.41	1.97	3.48	3.54	2.18	5.53	1.93	5.51	2.53
P ₂ O ₅	.21	.27	.21	.19	.24	.16	.16	.24	.19	.15	.23	.15	.23	.19
LOI	2.83	5.04	3.24	3.00	5.38	1.94	1.47	3.24	2.99	1.33	3.09	1.32	4.29	1.74
TOTAL	99.50	99.92	100.31	100.21	100.19	99.90	100.32	99.52	99.57	100.14	100.14	100.11	99.67	99.75
Rb	111	200	134	118	173	84	73	118	127	91	182	68	158	96
Sr	98	97	107	86	78	98	114	104	97	103	128	85	77	111
Ba	352	1167	547	525	1285	463	420	668	593	366	1160	383	1260	438
Y	39	45	44	37	42	34	38	41	33	36	42	30	39	40
Zr	242	248	224	198	196	184	241	208	163	199	202	167	196	178
Ce	94	89	78	116	62	83	93	92	95	89	103	67	83	74
La	37	41	63	54	75	56	66	71	64	54	73	48	65	49
Cu	65	35	26	71	34	36	16	32	33	41	43	27	16	21
Nb	11.7	16.0	13.1	11.4	15.1	10.4	9.8	12.9	10.6	8.8	15.3	8.7	13.8	9.3
Ni	28	48	32	27	40	28	19	38	37	20	43	18	51	26
Zn	82	121	85	76	106	78	54	100	99	60	99	55	117	75
Co	16	24	18	16	23	15	13	22	19	13	21	10	25	16
V	88	215	120	117	250	97	89	150	151	74	210	77	245	99
Cr	80	140	82	84	151	74	72	108	99	56	129	59	147	68

TABLE 2 (continued)

No.	3620	3621	3622	3623	3624	3625	3626	3631	3632	3633	3634	3638	3639	3640
L	3	3	3	3	3	3	3	5	5	5	5	6	6	6
R	s	g	g	s	s	g	s	g	s	g	s	s	g	s
P	6	7	7	7	7	8	8	10	10	11	11	14	12	12
S	D	M	M	M	M	D	D	D	D	D	D	M	D	D
SiO ₂	63.15	71.09	71.11	56.90	59.93	71.62	51.18	72.48	50.47	72.76	54.90	52.58	73.28	65.37
TiO ₂	1.03	1.21	1.15	1.03	1.03	1.15	1.24	1.02	1.26	.82	1.06	1.27	.86	.97
Al ₂ O ₃	14.87	11.46	11.42	18.27	17.31	11.18	22.42	11.49	21.61	11.67	20.89	21.13	11.09	13.86
FeO	7.10	5.71	5.58	7.76	7.50	5.45	8.32	5.01	8.47	4.46	7.02	8.42	4.79	6.31
MnO	.11	.09	.10	.12	.11	.10	.12	.10	.09	.07	.09	.11	.07	.09
MgO	3.50	2.32	2.22	4.41	4.29	2.26	4.37	2.37	4.82	2.03	3.91	4.31	2.21	3.02
CaO	1.63	1.74	1.98	.80	.69	1.86	.92	1.93	1.32	1.78	.82	.95	1.67	1.56
Na ₂ O	1.83	2.54	2.75	1.25	1.20	2.63	1.28	1.85	1.33	1.95	.85	.93	2.66	2.09
K ₂ O	3.61	2.04	1.84	4.53	4.12	1.97	5.78	2.01	6.44	2.02	6.66	5.39	1.97	3.29
P ₂ O ₅	.21	.21	.20	.18	.21	.21	.26	.19	.25	.17	.25	.21	.18	.24
LOI	2.43	1.61	1.70	4.17	3.88	1.34	4.46	1.60	3.71	1.57	3.75	5.15	1.11	1.84
TOTAL	99.47	100.02	100.03	99.41	100.26	99.75	100.32	100.04	99.76	99.29	100.17	100.44	99.87	98.64
Rb	153	82	74	155	132	87	167	81	208	90	222	185	80	130
Sr	121	120	120	67	54	122	81	102	115	109	81	90	143	140
Ba	595	368	342	812	753	315	1134	292	961	358	1323	1037	343	603
Y	38	50	46	43	41	46	37	41	53	36	41	46	39	47
Zr	175	348	315	178	176	312	213	282	242	193	190	210	216	214
Ce	81	104	107	111	88	87	98	90	119	93	88	101	73	98
La	54	67	67	71	54	46	59	59	89	58	70	92	53	67
Cu	52	17	14	72	58	16	24	47	16	45	14	33	21	27
Nb	13.2	12.5	12.5	13.4	12.3	12.0	15.9	12.0	15.0	10.5	15.7	15.9	9.8	12.6
Ni	40	25	23	50	46	23	54	23	54	21	46	51	21	39
Zn	99	66	61	126	122	65	112	71	135	62	115	128	61	89
Co	23	15	14	28	26	16	25	13	29	13	25	32	14	21
V	149	106	101	187	175	95	254	107	216	98	220	217	94	141
Cr	92	90	85	124	119	87	149	82	142	71	132	146	72	90

TABLE 2 (continued)

No.	3641	3642	3643	3644	3645	3650	3651	3652	3653	3654	3655	3656	3657	3658
L	6	6	6	6	6	7	7	7	7	7	7	7	7	7
R	g	s	g	s	g	g	g	s	g	s	g	s	g	s
P	13	13	14	14	14	15	15	15	16	16	17	17	18	18
S	D	D	M	M	M	C	C	C	D	D	D	D	C	C
SiO ₂	72.59	59.72	72.91	54.22	71.45	79.12	76.46	51.41	78.07	56.12	76.97	60.49	73.56	60.84
TiO ₂	.96	1.07	.79	1.19	1.03	.70	.80	1.51	.56	1.28	.67	1.10	.94	1.38
Al ₂ O ₃	11.00	17.51	11.02	19.48	11.40	8.63	10.37	21.63	9.13	19.81	9.72	17.18	11.14	17.81
FeO	4.83	6.97	4.37	8.24	5.23	3.29	4.03	8.08	3.36	7.71	3.30	7.28	4.58	6.35
MnO	.08	.10	.13	.10	.08	.10	.06	.11	.12	.11	.11	.08	.04	.06
MgO	2.16	3.81	1.91	4.35	2.13	1.09	1.27	3.03	1.22	2.92	1.34	2.97	2.17	3.10
CaO	1.35	1.00	2.78	.93	1.86	1.09	.51	.70	1.95	1.04	2.80	.58	1.40	1.71
Na ₂ O	2.70	1.75	2.26	.98	2.05	2.19	1.87	.72	2.20	.88	1.98	.57	2.50	2.37
K ₂ O	2.05	3.92	1.19	5.06	1.68	1.53	2.81	7.27	1.15	6.26	1.19	6.13	2.10	4.06
P ₂ O ₅	.19	.23	.16	.26	.19	.12	.13	.18	.09	.17	.10	.18	.18	.33
LOI	1.20	3.09	1.45	4.56	2.35	1.42	1.65	4.95	1.35	3.50	1.86	2.84	1.05	2.14
TOTAL	99.09	99.18	98.94	99.41	99.44	99.27	99.96	99.59	99.20	99.82	100.06	99.39	99.66	100.19
Rb	86	119	51	188	84	74	106	259	58	245	62	250	88	145
Sr	131	109	129	85	162	135	103	77	105	99	125	60	157	194
Ba	426	828	315	1012	357	542	812	1751	234	1047	250	983	470	1055
Y	41	47	37	43	42	28	23	48	28	21	27	30	35	54
Zr	261	206	193	210	291	255	232	312	162	281	209	241	253	357
Ce	86	93	73	92	90	95	99	192	92	83	77	71	86	128
La	58	71	51	75	45	69	64	129	72	76	60	53	57	88
Cu	26	43	24	46	24	14	13	38	19	55	15	64	7	13
Nb	11.2	14.0	9.3	15.4	11.2	21.8	25.0	56.7	17.8	42.0	14.6	30.4	11.4	17.1
Ni	21	43	21	51	25	16	19	49	18	25	16	34	23	39
Zn	62	108	57	128	66	34	43	93	39	96	37	93	26	52
Co	15	25	11	30	15	11	12	29	10	24	10	21	15	19
V	87	164	86	215	102	60	68	155	45	128	51	108	79	189
Cr	76	109	65	143	89	71	72	131	54	129	61	109	71	117

TABLE 3: Average analyses of gneisses and schists from different localities.

	A gneiss	B schist	C gneiss	D schist	E gneiss	F schist	G gneiss	H schist	I gneiss	J schist
L	1-6	1-6	7	7	1-6	1-6	1-6	1-6	1-6	1-6
S	all	all	all	all	M	M	D	D	C	C
SiO ₂	71.79	57.01	76.84	57.22	72.16	58.31	72.06	57.47	71.03	54.38
TiO ₂	.93	1.12	.73	1.32	.98	1.08	.95	1.11	.86	1.20
Al ₂ O ₃	11.71	18.85	9.80	19.11	11.34	17.92	11.50	18.53	12.40	20.73
FeO	5.03	7.44	3.71	7.36	5.09	7.52	5.01	7.36	5.00	7.42
MnO	.08	.10	.09	.09	.10	.11	.09	.10	.07	.09
MgO	2.23	3.90	1.42	3.01	2.16	4.02	2.27	3.90	2.28	3.70
CaO	1.58	1.04	1.55	1.01	1.79	.97	1.71	1.21	1.18	.87
Na ₂ O	2.28	1.29	2.15	1.14	2.39	1.26	2.36	1.52	2.07	1.00
K ₂ O	2.17	4.97	1.76	5.93	1.86	4.35	2.09	4.95	2.65	5.91
P ₂ O ₅	.18	.23	.12	.22	.18	.22	.19	.24	.18	.24
LOI	1.81	3.82	1.46	3.35	1.75	4.00	1.42	3.21	2.35	4.45
TOTAL	99.81	99.75	99.63	99.75	99.78	99.77	99.63	99.59	100.06	99.98
Rb	88	164	78	225	75	151	87	167	104	178
Sr	114	95	125	108	124	83	120	108	96	95
Ba	389	949	462	1209	378	813	362	907	435	1218
Y	40	42	28	38	41	41	41	44	37	42
Zr	238	202	222	298	262	191	240	207	206	211
Ce	88	93	90	119	92	97	84	96	89	84
La	55	68	64	87	59	71	54	68	51	64
Cu	32	36	14	43	22	46	29	29	46	32
Nb	10.8	14.2	18.1	36.6	11.0	13.4	10.8	14.4	10.7	15.1
Ni	24	46	18	37	24	46	23	46	25	46
Zn	67	113	36	84	64	117	66	110	72	111
Co	14	25	12	23	14	26	15	25	15	23
V	96	197	61	145	97	183	97	191	95	230
Cr	76	126	66	122	79	123	76	119	72	142

TABLE 4: Element ratios for gneisses and schists.

No.	L	R	P	S	Al/Ti	Y/Ti*10 ⁴	Zr/Ti*10 ⁴	Nb/Ti*10 ⁴	Zn/Ti*10 ⁴	V/Ti*10 ⁴
3601	1	g	1	C	12	66	408	20	138	148
3602	1	s	1	C	14	56	309	20	151	268
3603	1	g	1	C	13	75	381	22	145	204
3604	1	g	2	C	13	69	371	21	142	219
3605	1	s	2	C	17	61	284	22	154	363
3606	2	g	3	M	13	70	379	21	161	200
3607	2	g	3	M	10	70	447	18	100	165
3608	2	s	3	M	13	63	321	20	154	232
3609	2	s	3	M	15	61	302	20	183	280
3610	2	g	4	C	12	81	449	20	135	167
3611	2	s	4	C	15	61	293	22	144	305
3612	2	g	5	C	13	73	404	21	133	186
3613	2	s	5	C	16	57	287	20	171	358
3619	3	g	6	D	12	75	334	17	141	186
3620	3	s	6	D	13	62	283	21	160	241
3621	3	g	7	M	8	69	480	17	91	146
3622	3	g	7	M	9	67	457	18	88	146
3623	3	s	7	M	16	70	288	22	204	303
3624	3	s	7	M	15	66	285	20	198	283
3625	3	g	8	D	9	67	453	17	94	138
3626	3	s	8	D	16	50	287	21	151	342
3631	5	g	10	D	10	67	461	20	116	175
3632	5	s	10	D	15	70	320	20	179	286
3633	5	g	11	D	13	73	393	21	126	199
3634	5	s	11	D	17	65	299	25	181	346
3638	6	s	14	M	15	60	276	21	168	285
3639	6	g	12	D	11	76	419	19	118	182
3640	6	s	12	D	13	81	368	22	153	242
3641	6	g	13	D	10	71	454	19	108	151
3642	6	s	13	D	14	73	320	22	168	255
3643	6	g	14	M	12	78	408	20	120	182
3644	6	s	14	M	14	60	294	22	179	301
3645	6	g	14	M	10	68	471	18	107	165
3650	7	g	15	C	11	67	608	52	81	143
3651	7	g	15	C	11	48	484	52	90	142
3652	7	s	15	C	13	53	345	63	103	171
3653	7	g	16	D	14	83	483	53	116	134
3654	7	s	16	D	14	27	366	55	125	167
3655	7	g	17	D	13	67	520	36	92	127
3656	7	s	17	D	14	45	365	46	141	164
3657	7	g	18	C	10	62	449	20	46	140
3658	7	s	18	C	11	65	432	21	63	228

TABLE 5: Ratios between Ti, and Nb, P, La, Ce, Y, Fe, Al and Zr. Kuiseb Formation only.

No.	L	R	P	S	Nb/Ti·10 ⁴	P/Ti·10	La/Ti·10 ⁴	Ce/Ti·10 ⁴	Y/Ti·10 ⁴	Fe/Ti	Al/Ti	Zr/Ti·10 ⁴
3601	1	g	1	C	20	1.54	62	158	66	7	12	408
3602	1	s	1	C	20	1.47	51	111	56	8	14	309
3603	1	g	1	C	22	1.56	107	133	75	8	13	381
3604	1	g	2	C	21	1.55	101	217	69	7	13	371
3605	1	s	2	C	22	1.52	109	90	61	8	17	284
3606	2	g	3	M	21	1.44	115	171	70	8	13	379
3607	2	g	3	M	18	1.29	122	172	70	7	10	447
3608	2	s	3	M	20	1.62	110	142	63	8	13	321
3609	2	s	3	M	20	1.54	119	176	61	9	15	302
3610	2	g	4	C	20	1.48	122	201	81	8	12	449
3611	2	s	4	C	22	1.46	106	149	61	8	15	293
3612	2	g	5	C	21	1.58	116	162	73	8	13	404
3613	2	s	5	C	20	1.47	95	121	57	9	16	287
3619	3	g	6	D	17	1.55	92	139	75	8	12	334
3620	3	s	6	D	21	1.48	87	131	62	9	13	283
3621	3	g	7	M	17	1.26	92	143	69	6	8	480
3622	3	g	7	M	18	1.27	97	155	67	6	9	457
3623	3	s	7	M	22	1.27	115	180	70	10	16	288
3624	3	s	7	M	20	1.48	87	143	66	9	15	285
3625	3	g	8	D	17	1.33	67	126	67	6	9	453
3626	3	s	8	D	21	1.53	79	132	50	9	16	287
3631	5	g	10	D	20	1.36	96	147	67	6	10	461
3632	5	s	10	D	20	1.44	118	158	70	9	15	320
3633	5	g	11	D	21	1.51	118	189	73	7	13	393
3634	5	s	11	D	25	1.72	110	138	65	9	17	299
3638	6	s	14	M	21	1.20	121	133	60	9	15	276
3639	6	g	12	D	19	1.52	103	142	76	7	11	419
3640	6	s	12	D	22	1.80	115	169	81	8	13	368
3641	6	g	13	D	19	1.44	101	149	71	7	10	454
3642	6	s	13	D	22	1.56	110	145	73	8	14	320
3643	6	g	14	M	20	1.47	108	154	78	7	12	408
3644	6	s	14	M	22	1.59	105	129	60	9	14	294
3645	6	g	14	M	18	1.34	73	146	68	7	10	471
<u>Gneisses and schists</u>												
Mean =					20	1.5	101	150	68	8	13	363
Std. Deviation =					2	.13	18	25	7	1.0	2	70
Maximum =					25	1.8	122	217	81	10	17	480
Minimum =					17	1.2	51	90	50	6	8	276
<u>Gneisses only</u>												
Mean =					19	1.4	100	159	71	7	11	422
Std. Deviation =					1.6	.1	18	24	4	.7	1.7	41
<u>Schists only</u>												
Mean =					21	1.5	102	140	64	9	15	301
Std. Deviation =					1.3	.1	18	23	7	.6	1.3	23

TABLE 6: K-Rb-Ba ratios. Kuiseb metasediments.

No.	L	R	P	S	K/Rb	K/Ba	Ba/Rb
3601	1	g	1	C	206	65	3.2
3603	1	g	1	C	208	51	4.1
3604	1	g	2	C	214	48	4.4
3606	2	g	3	M	238	43	5.5
3607	2	g	3	M	224	39	5.8
3610	2	g	4	C	199	49	4.0
3612	2	g	5	C	236	42	5.6
3619	3	g	6	D	219	48	4.6
3621	3	g	7	M	206	46	4.5
3622	3	g	7	M	206	45	4.6
3625	3	g	8	D	188	52	3.6
3631	5	g	10	D	206	57	3.6
3633	5	g	11	D	186	47	4.0
3639	6	g	12	D	204	48	4.3
3641	6	g	13	D	198	40	5.0
3643	6	g	14	M	194	31	6.2
3645	6	g	14	M	166	39	4.3
3602	1	s	1	C	255	44	5.8
3605	1	s	2	C	310	42	7.4
3608	2	s	3	M	245	43	5.7
3609	2	s	3	M	231	50	4.7
3611	2	s	4	C	252	40	6.4
3613	2	s	5	C	289	36	8.0
3620	3	s	6	D	196	50	3.9
3623	3	s	7	M	243	46	5.2
3624	3	s	7	M	259	45	5.7
3626	3	s	8	D	287	42	6.8
3632	5	s	10	D	257	56	4.6
3634	5	s	11	D	249	42	6.0
3638	6	s	14	M	242	43	5.6
3640	6	s	12	D	210	45	4.6
3642	6	s	13	D	273	39	7.0
3644	6	s	14	M	223	42	5.4
Mean							
Gneisses					206	46	4.5
Schists					251	44	5.8
Standard Deviation							
Gneisses					18	8	.8
Schists					29	5	1.1